

# SELF-ACTIVATING NEURAL ENSEMBLES FOR CONTINUAL REINFORCEMENT LEARNING

**Sam Powers**

Carnegie Mellon University  
snpowers@cs.cmu.edu

**Eliot Xing**

Georgia Institute of Technology  
exing@gatech.edu

**Abhinav Gupta**

Carnegie Mellon University  
gabhinav@cs.cmu.edu

## ABSTRACT

The ability for an agent to continuously learn new skills without catastrophically forgetting existing knowledge is of critical importance for the development of generally intelligent agents. Most methods devised to address this problem depend heavily on well-defined task boundaries, and thus depend on human supervision. Our task-agnostic method, Self-Activating Neural Ensembles (SANE), uses a modular architecture designed to avoid catastrophic forgetting without making any such assumptions. At the beginning of each trajectory, a module in the SANE ensemble is activated to determine the agent’s next policy. During training, new modules are created as needed and only activated modules are updated to ensure that unused modules remain unchanged. This system enables our method to retain and leverage old skills, while growing and learning new ones. We demonstrate our approach on visually rich procedurally generated environments.

## 1 INTRODUCTION

Lifelong learning (Thrun & Mitchell, 1995) is of critical importance for the field of robotics. An agent that interacts with the world should continuously learn from it and act intelligently in a wide variety of situations. In contrast to this ideal, most standard deep reinforcement learning methods are centered around a single task. First, a task is defined, then a policy is learned to maximize the rewards the agent receives in that setting. If the task is changed, a new model is learned from scratch, discarding the previous model and previous interactions. Task specification thus plays a central role in current end-to-end deep reinforcement learning frameworks.

In contrast, humans do not require concrete task boundaries to be able to effectively learn separate tasks—instead, we perform continual (lifelong) learning. We learn new skills efficiently by leveraging prior knowledge, without forgetting old behaviors. However, when placed into continual learning settings, current deep reinforcement learning approaches do neither: the forward transfer properties of these systems are negligible, and they suffer from catastrophic forgetting (McCloskey & Cohen, 1989; French, 1999).

The core issue of catastrophic forgetting is that a neural network trained on one task starts to forget what it knows when trained on a second task, and this issue only becomes exacerbated as more tasks are added. The problem ultimately stems from sequentially training a single network in an end-to-end manner. The shared nature of the weights and the use of backpropagation to update them mean that later tasks overwrite earlier ones (McCloskey & Cohen, 1989; Ratcliff, 1990).

To handle this, past approaches have proposed a wide variety of ideas: from task-based regularization (Kirkpatrick et al., 2017), to learning different sub-modules for different tasks (Rusu et al., 2016), and dual-system slow/fast learners inspired by the human hippocampus (Schwarz et al., 2018). The fundamental problem of continual learning, which few methods address, is that the agent should autonomously determine how and when to adapt to changing environments, or stabilize existing knowledge, without explicit task specification. It is infeasible for a human to indefinitely provide agents with task-boundary supervision, and doing so side-steps the core problem.

There are a few existing task-agnostic (Zeno et al., 2018) methods, though most have only been demonstrated on classification or behavior cloning: for example Aljundi et al. (2019b) addresses the problem by detecting plateaus and using those as boundaries, Lee et al. (2019) adaptively creates new clusters using Dirichlet processes, and Veness et al. (2021) replaces backpropagation completely. Methods that have been demonstrated on reinforcement learning are rarer; exceptions include Rolnick et al. (2019), which utilizes a large replay buffer, and Lomonaco et al. (2020) which uses the error in the value estimate to determine when to consolidate modules.

We approach the problem by introducing a system that continuously, dynamically adapts to changing environments. Our ensemble-based method, Self-Activating Neural Ensembles<sup>1</sup> (SANE), depicted in Figure 1, is the core of our proposal. Each module in the ensemble is a separate, task-agnostic network. Periodically, a single module from the ensemble is activated to determine which policy to use. Only activated modules are updated, leaving unused modules unchanged and therefore protected from catastrophic forgetting. Crucially, our ensemble is dynamic: new modules are created when existing modules are found to be insufficient. In this way, modules are created when novel scenarios are encountered, preventing destructive updates to other modules. Additionally, SANE is simple; modules control their own relevance, activating when the situation to which they are specialized is encountered, and remaining untouched the rest of the time. SANE provides the following desirable properties for continual reinforcement learning: (a) It mitigates catastrophic forgetting by only updating relevant modules; (b) Because of its task-agnostic nature, unlike previous approaches, it does not require explicit supervision with task IDs; (c) It achieves these targets with bounded resources and computation. We demonstrate SANE on three visually rich, challenging level sequences based on Procgen (Cobbe et al., 2020) environments. Additionally, we analyze the behavior of SANE at a more fine-grained level on 2 individual runs, to gain more understanding of the dynamics of training SANE.

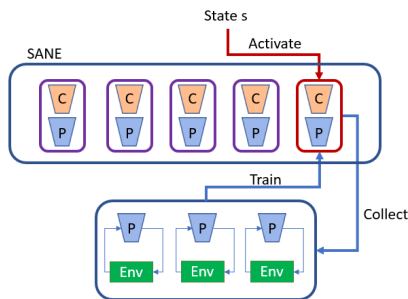


Figure 1: The overall structure of the SANE system. Each module contains an actor and a critic. Upon activation, collection occurs from several environments in parallel.

## 2 RELATED WORK

**Continual learning** Any continual learning system must balance *stability* (the extent to which existing knowledge is retained) and *plasticity* (how readily new knowledge is acquired) (Grossberg, 1982; Abraham & Robins, 2005; Mermillod et al., 2013). Stability has posed a substantial challenge due to *catastrophic forgetting*, by which neural networks trained by backpropagation abruptly forget learned behavior for solving old tasks when presented with new tasks (Kemker et al., 2018; McCloskey & Cohen, 1989; Ratcliff, 1990; Lewandowsky & Li, 1995; French, 1999). Broadly, methods for continual learning can be categorized under Regularization, Rehearsal, or Architectural approaches, as well as combinations of them. We refer the reader to the survey papers by Parisi et al. (2019); Lesort et al. (2020); Mundt et al. (2020) for general discussion. Here we review methods for continual learning relevant to our approach.

Recent strategies for mitigating catastrophic forgetting such as Elastic Weight Consolidation (EWC) (Kirkpatrick et al., 2017), among other Regularization approaches (Lee et al., 2017b; Li & Hoiem, 2017; Zenke et al., 2017; Ritter et al., 2018; Chaudhry et al., 2018a; Jaeger, 2017; He & Jaeger, 2018; Serra et al., 2018; Aljundi et al., 2018; 2019b; Park et al., 2019), constrain updates to network parameters important for past tasks when learning new tasks. However, these methods fundamentally run into the stability-plasticity dilemma, as over-constraining updates can hinder the learning of new tasks. To improve plasticity, dynamic architectures (Ring, 1998; Zhou et al., 2012; Terekhov et al., 2015; Rusu et al., 2016) incorporate additional network parameters to help learn new tasks. Furthermore, to prevent model size from growing unbounded, such approaches (Xiao et al., 2014; Cortes et al., 2017; Yoon et al., 2018; Mallya et al., 2018; Mallya & Lazebnik, 2018; Xu & Zhu, 2018; Schwarz et al., 2018; Kaplanis et al., 2019; Traoré et al., 2019) use distillation (Buciluă et al., 2006; Hinton et al., 2015; Rusu et al., 2015; Teh et al., 2017), pruning, and related techniques to consolidating learned behavior while reducing parameter count. Similarly, Rehearsal and (generative) memory-based approaches (Robins, 1995; French, 1997; Gepperth & Karaoguz, 2016; Furlanello et al., 2016; Rebuffi et al., 2017; Shin et al., 2017; Draelos et al., 2017; Kamra et al., 2017; Lopez-Paz & Ranzato, 2017; Chaudhry et al., 2018b; Wu et al., 2018; Isele & Cosgun, 2018; Parisi et al., 2018; Riemer et al., 2018; Soltoggio et al., 2018; Kemker & Kanan, 2018; Van de Ven & Tolias, 2018; Xiang et al., 2019; Aljundi et al., 2019a; Lesort et al., 2019;

<sup>1</sup>Code available: [https://github.com/AGI-Labs/continual\\_rl](https://github.com/AGI-Labs/continual_rl)

Caccia et al., 2020; Caselles-Dupré et al., 2021) must also balance data storage and memory network constraints when determining which examples are needed to preserve previously learned behavior. We build our ensemble approach off of CLEAR (Rolnick et al., 2019), a state-of-the-art asynchronous continual RL method which uses Rehearsal, by maintaining a replay buffer that uniformly preserves past experience via reservoir sampling (Isele & Cosgun, 2018), along with Regularization, via behavioral cloning and a KL penalty to preserve prior learned behavior.

**Ensemble methods** Falling under Architectural approaches, aggregation ensembles (Cheung et al., 2019; Wen et al., 2020; Veness et al., 2021) combine predictions from multiple models to produce a final output. These types of ensembles are also commonly used for uncertainty estimation (Lakshminarayanan et al., 2017), exploration (Pathak et al., 2019), or reducing overestimation bias such as in double Q-learning (Van Hasselt et al., 2016; Fujimoto et al., 2018). In contrast, modular ensembles (Aljundi et al., 2017; Fernando et al., 2017; Lee et al., 2019; Parascandolo et al., 2018; Kessler et al., 2021) use a subset of the entire ensemble’s parameters to select an appropriate expert model for the task presented. Selectively updating a subset of parameters or specific modules instead of the entire ensemble can circumvent catastrophic forgetting while bounding compute costs; this is a feature we utilize in SANE, which is a type of modular ensemble rather than the former, aggregation ensemble. Our method is similar to Multiple Choice Learning (Guzman-Rivera et al., 2012; Lee et al., 2016; 2017a; Seo et al., 2020), which chooses and updates only the best expert from an ensemble, encouraging specialization. However, Multiple Choice Learning uses fixed-size static ensembles, while SANE is a dynamic ensemble that merges similar modules and works with a given resource budget. For supervised continual learning, LMC (Ostapenko et al., 2021) also proposes a modular ensemble approach, although LMC assumes access to task IDs at training time and can only add modules, meaning that its computational footprint is linear relative to the number of tasks learned. In contrast, SANE is completely task-agnostic at train and test time, while also creating and merging modules to meet a given compute budget.

Hierarchical RL can be seen as a hierarchy of meta-policies that control access to an ensemble of (often hand-designed) sub-policies that act at differing temporal resolutions (Sutton et al., 1999; Brunskill & Li, 2014; Tessler et al., 2017; Zhang et al., 2021). Analogous to our own value-based activation score, some hierarchical RL methods use predicted Q-values to select amongst their ensemble, as in (Dayan & Hinton, 1992; Dietterich, 2000). Goyal et al. (2019) demonstrates the utility of avoiding meta-policies, instead relying on primitives that independently determine their own relevance, similar to self-activation in our approach. However, their primitives distinguish themselves by factorizing a state space, placing strong assumptions on the learnable policies. Additionally, their primitives are not created over time, so the method relies on regularization to ensure primitives in their ensemble are used.

### 3 BACKGROUND

We review background on the continual RL setting we study in Appendix A.7. Traditional neural networks suffer from catastrophic forgetting because weights in the network are changed by backpropagation every update (McCloskey & Cohen, 1989), causing information learned in a new scenario to overwrite prior behavior. Instead of learning and updating a single neural network for policy  $\pi$  across multiple tasks, we propose using an dynamic ensemble of *self-activating modules*. Our approach partitions, allocates, and manages parameters for separate modules, so that each module may handle different situations without interfering with others.

If a module is relevant to the current situation, it activates during inference and is updated during training. If a module is irrelevant, it is unused and remains unchanged. One way of viewing these modules is as latent behaviors, each specialized to a particular circumstance. For example, if in one context an agent must carefully wait to allow an enemy to pass, we don’t want this to disrupt a behavior where moving quickly to dodge an enemy is the best action.

How may we know when to use which module, when task boundaries are ambiguous and not given by human supervision? Each module in our ensemble predicts an *activation score*, which estimates the relevancy of a given module’s behavior to the current situation, and the module with the highest activation score is selected from the ensemble. An appropriate activation score will protect modules against catastrophic forgetting, and can also enable forward transfer, by activating modules with prior learned behaviors that are advantageous in new settings.

How should such an ensemble be structured? Pre-defining a static fixed-size ensemble is ineffective for module-based behavior specialization. In such a static ensemble, one module will tend to perform well at a task, leading to that module being chosen as the starting point for future tasks which results in catastrophic forgetting. Regularizing with additional losses would be necessary to distribute activation across the ensemble’s experts, as in (Jacobs et al., 1991; Shazeer et al., 2017; Goyal et al., 2019). Instead, we design SANE as a *dynamic ensemble*, in which modules are created and merged together as necessary. Intuitively, modules are created when existing latent behaviors fail to perform as expected, and the ensemble determines that a new latent behavior is needed. Modules may also be merged to conserve resource consumption and meet a given compute budget.

Bringing self-activating modules and a dynamic ensemble together, we present Self-Activating Neural Ensembles (SANE). To summarize, our approach differs from traditionally-used ensembles in two ways: (i) We do not aggregate results across modules, in order to keep modules isolated from one another. This circumvents catastrophic forgetting, by not backpropogating through the entire ensemble. (ii). The ensemble itself is dynamic, in that modules are being created and merged throughout training.

## 4 SELF-ACTIVATING NEURAL ENSEMBLES FOR CONTINUAL RL

We now proceed to formally describe SANE in full detail. SANE is a dynamic collection of modules  $\{M_1, \dots, M_k\}$  where, based on the context, one module  $M_t$  activates and is used for inference. Subsequently, given transitions from collected episodes, only the selected module  $M_t$  is updated. We describe an individual SANE module in Section 4.1, including how activation scores are computed to determine which module to use. We present the learning process to manage a dynamic ensemble in Section 4.2. Pseudocode is provided in Appendix A.4.

### 4.1 SELF-ACTIVATING MODULE

Every module  $M_i$  is an actor-critic algorithm represented by: a policy  $\pi_i(a|s)$ , a critic  $V_i(v, u|s)$ , as well as a replay buffer  $\mathcal{B}_i$  that holds experience transitions. We modify the critic  $V_i$  from the standard formulation in the following way. Given a state  $s$  at timestep  $t$ , the critic  $V_i$  predicts two scalars:  $v_i(s)$ , the value estimate of the return  $R_t$  received if module  $M_i$  is activated, and  $u_i(s)$ , an uncertainty estimate of the absolute error:

$$u_i(s) \approx |R_t - v_i(s)| \quad (1)$$

We proceed by defining an optimistic estimate  $v_i^{UCB}$  (upper confidence bound) and a pessimistic estimate  $v_i^{LCB}$  (lower confidence bound) for the return that the module  $M_i$  can achieve from state  $s$ :

$$v_i^{UCB}(s) = v_i(s) + \alpha_u * u_i(s) \quad (2)$$

$$v_i^{LCB}(s) = v_i(s) - \alpha_l * u_i(s) \quad (3)$$

where  $\alpha_u, \alpha_l > 0$  are hyperparameters which represent how wide a margin around the expected value to allow. We use these margins to: (i) choose which module to activate during inference; (ii) decide when to create a new module during Structure Update (Section 4.2).

In all, each module  $M_i$  can be considered to be a tuple  $\langle \pi_i, V_i, \mathcal{B}_i, \bar{V}_i, A_i \rangle$ , where  $\bar{V}_i$  and  $A_i$  are two other versions of the critic  $V_i$ , which we proceed to describe.

The target network  $\bar{V}_i$  is used for the confidence bounds estimates (Equation 2 and 3) instead of  $V_i$ . Target networks are commonly used in Q-learning (Mnih et al., 2015; Lillicrap et al., 2016; Ansel et al., 2017; Fujimoto et al., 2018) to stabilize training by reducing variance from approximation error. Similarly, we update  $\bar{V}_i$  with an exponential moving average (Ruppert, 1988; Polyak & Juditsky, 1992; Izmailov et al., 2018). We denote  $V_i$ 's parameters by  $\theta_i$ ,  $\bar{V}_i$ 's parameters by  $\theta'_i$ , and the update rate by  $\tau_V$ ; we use the update:  $\theta'_i \leftarrow \tau_V \theta_i + (1 - \tau_V) \theta'_i$ .

The anchor  $A_i$  is a frozen instance of the critic  $V_i$  from when the module  $M_i$  was created. We describe how we use the anchor  $A_i$  to measure drift in Section 4.2.1.

**Module update** SANE can be applied to any actor-critic algorithm; we describe the specifics of our implementation in Section 4.4. Let  $L_{M_i}$  denote the loss function of the active SANE module and  $L_{rl}$  be the loss of the actor-critic RL algorithm, with components associated with module  $M_i$ . We perform a module update by optimizing  $L_{M_i} = L_{rl} + \mu L_{ue}$ , where  $L_{ue}$  is MSE loss to estimate uncertainty from Equation 1.

**Inference (Self-Activation)** SANE consists of several modules where each module represents the behavior for a particular situation. Activating the right module for the right situation is key to the success of the SANE method. In an RL setting, the critic predicts a value estimate, which can serve as an effective proxy for how successful a module  $M_i$  may be in obtaining high return. At the beginning of the episode, we compute  $v_i^{UCB}$  for each module in the ensemble  $\{M_1, \dots, M_k\}$  using the target network critic  $\bar{V}_i$ . Then, we greedily select the module whose critic predicts the highest such value, and use that module for the whole episode.

### 4.2 DYNAMIC ENSEMBLE

We propose a process to dynamically update the structure of the ensemble in SANE. If the current set of modules behave in an expected manner (returns are within the expected range) then the current set is sufficient. However

at some point in training, if the returns are outside the expected range, then we know the current set of modules is insufficient. We create new modules to handle the new situation, and merge modules together to stay within a given compute budget.

#### 4.2.1 MEASURING DRIFT

The key to successfully updating the SANE structure lies in our ability to detect that we have moved outside this expected range. Our main assumption here is that the change in rewards received is sufficient for distinguishing relevant changes in setting. Therefore, we detect change in setting by measuring drift in rewards. Drift describes when an environment is non-stationary, e.g. when the reward distribution or the state transition distribution is changing over time. Often where drift occurs, catastrophic forgetting follows because networks update to the new setting, forgetting the old.

To recognize drift with SANE, at the time of their creation modules have their critic cloned and frozen, creating a static critic called the *anchor*. We compare the prediction of a module’s critic to the prediction of its anchor. We say that sufficient change has occurred when the bounds of the expected return, as defined in Section 4.1, predicted by a module’s critic do not include the value predicted by its anchor, which serves as a static baseline.

Let  $v_{A_i}$  denote the value estimate of the anchor  $A_i$ . Formally, we say that sufficient change has occurred when for a given state  $s$ , critic  $V_i$ , and anchor  $A_i$ , either of the following inequalities hold:

$$v_i^{UCB}(s) < v_{A_i}(s) \tag{4}$$

$$v_i^{LCB}(s) > v_{A_i}(s) \tag{5}$$

In practice, we use the target network critic  $\bar{V}_i$  to predict  $v_i^{UCB}(s)$  and  $v_i^{LCB}(s)$ , instead of  $V_i$ .

#### 4.2.2 CREATING A NEW MODULE

When drift occurs such that the returns are better than anticipated, we expect that this corresponds to the case that the policy has simply improved in the current setting, as intended by standard module policy training. In this setup, we just update the anchor to improve expectation. However, the case of negative drift, where the UCB falls below the estimate of the anchor, requires a different strategy. This situation occurs when the behavior (policy) starts under-performing expectation, which can occur when the task has been changed and the old policy is no longer as effective as it had been. What we do in this case is create a new module that is a clone of the one that was activated. We empty the replay buffer and update the anchor at the time of creation of the new module. The goal is for the new module to be activated by the new setting while the old one continues to be activated by the old setting, splitting the input space to more effectively handle the two desired behaviors that are not well handled by a single policy.

#### 4.2.3 MERGING MODULES

To prevent unlimited memory consumption, we limit the the total number of modules in our ensemble by merging modules. To execute a merge, we start by finding the two modules in the ensemble that are closest by the L2 distance between frames averaged from a sample of trajectories from the replay buffers. We then keep the more frequently used module and drop the less frequent module from the ensemble. Before dropping, we combine the replay buffer of the two modules and run a module update (Section 4.1) on the combined module.

Note that in combining the replay buffers of the two modules we use the reservoir sampling technique from CLEAR (Rolnick et al., 2019). We maintain a reservoir value for each trajectory, defined as a random value between 0 and 1, that allows every trajectory to have an equal chance of being stored in the buffer, regardless of when it was collected. The trajectories from the module being dropped are added to the replay buffer of the module being kept using the reservoir values that were originally generated.

### 4.3 IMPLEMENTATION DETAILS

**Leveraging CLEAR and IMPALA** We have chosen to base our modules on IMPALA-based CLEAR as implemented by CORA (Powers et al., 2021), as it allows us to get several useful features for free: a. Learning is done efficiently, in a highly parallel manner. b. The expected return, used for training both the critic and the policy (for SANE as well as all baselines), is computed using vtrace, an effective credit assignment method, as described in (Espoholt et al., 2018). c. The CLEAR replay buffers are maintained using reservoir sampling. d. CLEAR provides auxiliary losses that maintain consistency of both the policy and critic with the replay buffer.

**Model architecture** The base implementation uses the Nature CNN model from Mnih et al. (2015). We augment the baseline network with 2 hidden linear layers of dimension 32 with ReLU nonlinearities to increase its representational capacity. All other hyperparameters for the experiments are provided in Appendix A.1. Our code is provided in additional materials, and will be open sourced upon publication.

**Parallelism** By collecting data from multiple environments in parallel, training is considerably faster, but it requires us to make one key assumption: the activated module must be guaranteed to be applicable to all actors being run at the same time. This requires that all actors be running the same task.

## 5 EXPERIMENTS

**Task sequences** We choose three procedurally-generated game environments (Climber, Miner, Fruitbot) from Progen (Cobbe et al., 2020). We construct three task sequences using each of these game environments, by isolating sequences of levels that are likely to cause catastrophic forgetting and where approaches like CLEAR would perform poorly. We selected four levels for Climber and Miner. For Fruitbot, we added an easier fifth level at the start as a simple curriculum. We run each set of levels for three cycles, to see how learning evolves as the levels are seen again. The first frame of the selected levels are visualized in Figure 2.

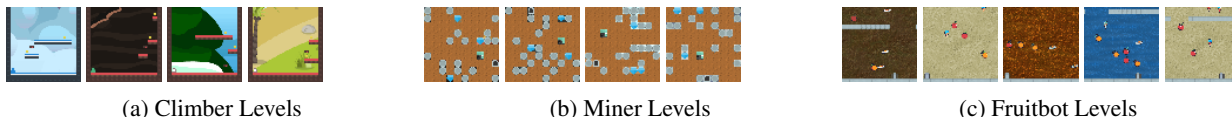


Figure 2: The first frame of each sequence of levels used in our experiments.

**Baselines** We compare our approach to three baselines. We also perform an ablation showing the importance of the dynamic ensemble compared to a static set. The baselines we selected are:

- **CLEAR** We compare to CLEAR (Rolnick et al., 2019), a state-of-the-art continual RL method (Powers et al., 2021). In addition to comparing to CLEAR with the default number of parameters (the same as each module in the SANE ensemble), we also compare to a version of CLEAR with as many total parameters as we use in our SANE ensemble. We refer to this as “CLEAR 8x”.

Note that while SANE takes around 14 hours to run our Fruitbot sequence and standard CLEAR takes around 10 hours, these larger models take longer to run: CLEAR 8x took 4.5 days. We would have liked to compare to a CLEAR 32x as well, but such an experiment was on track to take more than 2 weeks. This exemplifies another benefit of SANE: the effective usage of more parameters without such a dramatic increase in runtime.

- **Elastic Weight Consolidation (EWC)** We compare to EWC (Kirkpatrick et al., 2017), which uses the diagonal of the Fisher matrix to estimate the importance of parameters for past tasks, and slows updates to those parameters when learning new tasks.
- **Progress & Compress (P&C)** We additionally compare to P&C (Schwarz et al., 2018), which uses an online variant of EWC to consolidate learned behavior between dual networks, after each task is learned.
- **Static SANE Ensemble** To validate the utility of our dynamic SANE ensemble, we compare to a SANE ensemble that is static: all modules are initialized upfront, and no creation or merging occur.
- **SANE Oracle** We also compare against an Oracle version of SANE, where each task has its own pre-specified module, which is looked up by task ID.

**Experimental setup & metrics** All hyperparameters for the methods used are given in the Appendix A.1. For fairness of comparison we hold constant the number of replay frames each method has access to in total, at 400k frames.

All implementations for baselines are based on those provided by (Powers et al., 2021). We use Continual Evaluation to generate plots for each task in the task sequence, which show how well each task was learned and how well each task was remembered. Every method was run for 5 seeds, and the mean and standard error of the mean are shown in the graphs. Gray shaded rectangles show when the agent trains on each task. We also report the Forgetting metric introduced in (Powers et al., 2021). We reproduce the definition of their Forgetting metric here.

$$r_{i,j,end} \quad \text{expected return achieved on task } i \text{ after training on task } j \quad (6)$$

$$r_{i,all,max} \quad \text{maximum expected return achieved on task } i \text{ after training on all tasks} \quad (7)$$

	SANE	Static SANE	CLEAR	CLEAR 8x	EWC 8x	P&C 8x	SANE Oracle
Climber	4.4 ± 1.0	5.3 ± 0.5	7.7 ± 0.1	8.1 ± 0.2	0.4 ± 0.3	1.5 ± 0.8	-0.6 ± 0.1
Miner	-0.2 ± 0.2	1.4 ± 1.1	6.3 ± 0.3	6.3 ± 0.2	4.1 ± 0.8	0.1 ± 0.1	-0.9 ± 0.4
Fruitbot	5.5 ± 0.7	5.8 ± 0.3	7.6 ± 0.4	6.3 ± 0.6	3.7 ± 0.7	1.6 ± 0.1	0.3 ± 0.1

Table 1: Forgetting ( $\mathcal{F}$ ) summary statistics for all experiments. EWC and P&C exhibit little forgetting because they also exhibit little learning. Of the methods that learned the tasks, we see SANE performs best.

Forgetting compares the maximum final expected return achieved for a task  $i$  at any prior point to the expected return while training on task  $j$ , where  $j > i$ :

$$\mathcal{F}_{i,j} = \frac{10}{s} \sum_s \left( \frac{r_{i,j,end} - r_{i,j-1,end}}{|r_{i,all,max}|} \right)$$

We compute the Forgetting statistic for only the first cycle for each seed and take the average across tasks. We report the average and standard error of the mean across seeds for the Forgetting summary statistic.

## 5.1 RESULTS

We present the Forgetting summary statistics (Powers et al., 2021) for all methods in Table 1 and the Continual Evaluation graphs, which present the average and standard error of the mean of the returns received from the environment versus steps taken in the environment, in each section. We also present the final average performance and standard error of the mean for all benchmarks in the Appendix, Tables 3-5.

**Climber:** First we demonstrate SANE on Climber, a side-view task where the agent must ascend a series of platforms while collecting coins and dodging bats. The selected levels are particularly challenging because avoiding the bats requires relatively precise timing; a slight decay in policy performance results in significantly reduced reward.

We start by analyzing the Continual Evaluation results in Figure 3. SANE and Static SANE both learn the tasks, but we can see that our dynamic model consistently learns and remembers, while Static SANE overall shows more inconsistent performance, doing particularly poorly on Envs 0 and 2. Both versions of CLEAR learn the tasks but readily forget them, indicating that SANE is not improving by merely adding more parameters. EWC has mixed results; it does worse than SANE uniformly on all cycles of Env 0 and the first cycle of the other Envs, but approximately ties it on the other cycles of Envs 2 and 3, and exceeds it on the other cycles of Env 1. P&C largely fails to learn the tasks at all, with some exception on Env 2.

These results are further validated by looking at the Forgetting summary statistics presented in Table 1. By this metric EWC does the best, likely aided by poorer learning during the first cycle of Envs 0 and 1 and the particularly good later performance on Env 1. Of the four methods that learned all tasks immediately (SANE, Static SANE, CLEAR, and CLEAR 8x), SANE exhibits the least forgetting.

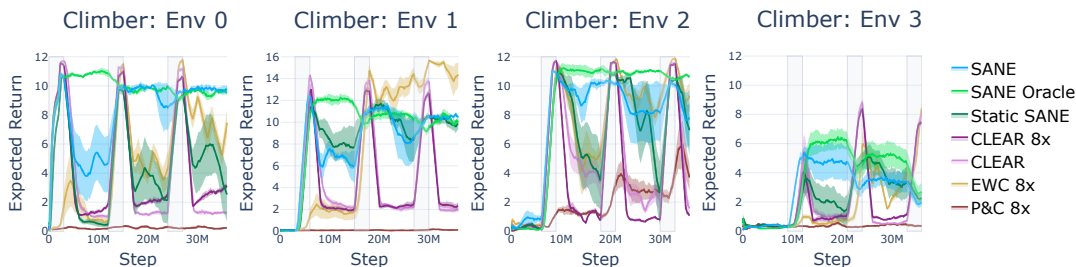


Figure 3: Results for Continual Evaluation on the Climber sequence of tasks. We observe that SANE consistently learns and recalls the tasks. Gray shaded rectangles show when the agent trains on each task.

**Miner:** We additionally demonstrate SANE on Miner, a task where the agent must dig through dirt in two dimensions, collecting diamonds and going to a specified end-goal without getting crushed by rocks.

Continual Evaluation results are shown in Figure 4. SANE overall outperforms the baselines on the first three environments; we see CLEAR and EWC learning and forgetting, static SANE showing more recall than CLEAR but less than SANE, and largely little learning from P&C with the exception of Env 1. However, on Env 2 one of SANE’s seeds fails to learn the task, and on Env 3 all seeds did. Perhaps CLEAR’s larger buffer effectively provides more exploration, as there is more randomness amongst the batches selected to be trained upon.

Table 1 again demonstrates numerically these qualitative results. We see that of the methods that learned the tasks, SANE not only did the best, it also exhibited some backwards transfer (negative forgetting).

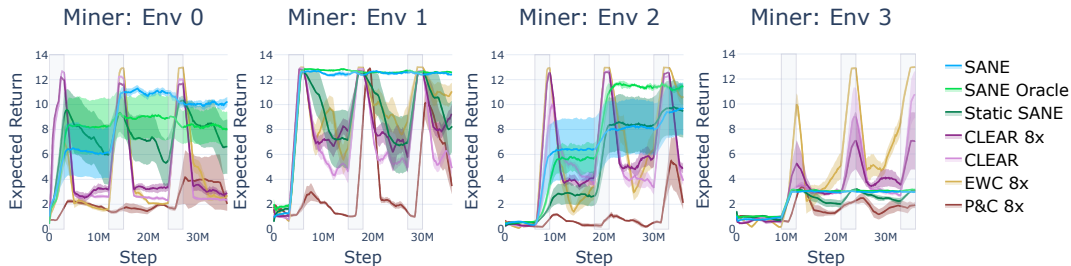


Figure 4: Results for Continual Evaluation on the Miner task sequence. We again observe that SANE improves on the baselines at recall across the tasks. Gray shaded rectangles show when the agent trains on each task.

**Fruitbot:** The final Procggen sequence we use is based on Fruitbot, where the environment continuously scrolls and the agent must move left and right to collect fruit, avoid vegetables, and make it through gaps in the wall. Continual Evaluation results, shown in Figure 5, are less clear-cut than the previous two experiments. SANE clearly exceeds baselines on recall on Envs 1 and 3, but remains comparable to the CLEAR 8x baseline on Envs 2 and 4, and struggles on Env 0, only exceeding the baseline in the final cycle. Furthermore for the most part SANE receives a lower maximum score than the CLEAR baselines, with the exception of Env 3. Table 1 shows that despite the mixed qualitative results, SANE again exceeds baselines quantitatively.

## 6 ANALYSIS OF SANE

We generate two additional figures to help us analyze our SANE ensembles. The first is a *module ID* plot. On creation we assign every module a unique identifier: an integer that increases per module created. This ID is constant through the lifetime of the module, including when other modules get merged into it. We can plot what module is active by plotting its module ID. This allows us to see when there are periods of rapid creation (steep regions of the graph), when older modules are re-used, and when modules are being stably activated.

The second plot is a *lineage* plot, showing a graph that represents the history of the ensemble, with each node in the graph representing a module. A blue line indicates that one module spawned another, and a red line indicates that a module was merged into another. Light blue nodes represent modules that are current available to be activated at the current time. An example lineage plot<sup>2</sup> is shown in Appendix A.3.

### 6.1 SINGLE RUN: CLIMBER

We start by analyzing a single (non-hand-picked) run of SANE in Climber, to demonstrate the dynamics of learning in a simple environment where behaviors are readily separable. In Figure 6, we aligned a graph of the ID of the currently active module with the reward received at that time.

We can see the desired behavior in this case: several new modules are created (a sharp increase in module ID is observed) as performance successively fails to meet expectation, until a suitable module is created. Additionally, we can observe that before a task is trained upon, it is likely to use the best module for the current task. E.g. Env 3 uses Env 0’s active module (module 0) for the first 3M steps, then Env 1’s module (15) for most of the next 3M, then Env 2’s module (18) for the next 3M, until during its own training period drift is detected and a custom module is created.

It is also worth remarking on the decline in Env 3’s performance, which occurs particularly while the task is being trained. It occurs while a consistent module is being activated, so is not related to the ensembling behaviors of module

<sup>2</sup>An interactive lineage plot can also be viewed at [https://github.com/AGI-Labs/continual\\_rl](https://github.com/AGI-Labs/continual_rl).



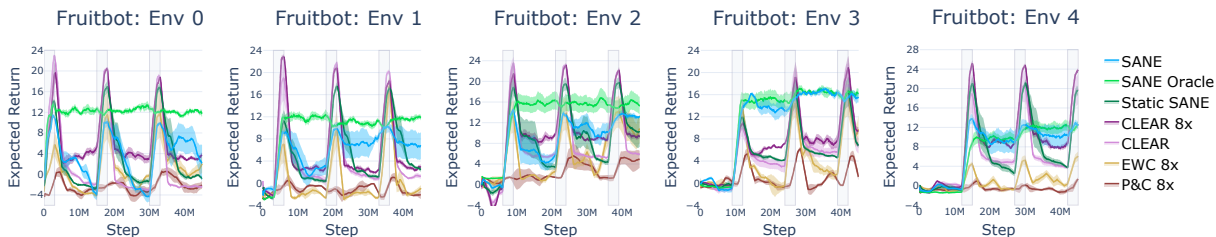


Figure 5: Results on the Fruitbot sequence. SANE performs particularly well on Envs 1 and 3, comparable to CLEAR 8x on Envs 2 and 4, and struggles some with Env 0. Gray shaded rectangles show when the agent trains on each task.

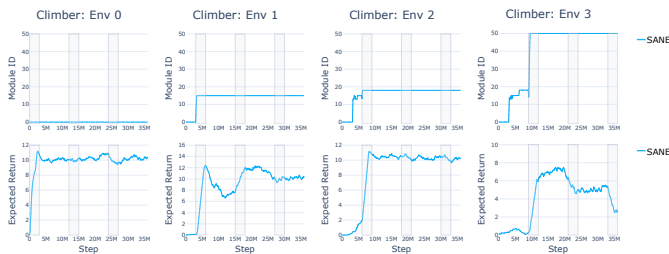


Figure 6: Module ID and expected return plots aligned by timestep, to show module activation during a single run of Climber. Gray shaded rectangles show when the agent trains on each task.

creation or merging. Observing the behavior indicates that the agent is jumping into a bat rather than avoiding it, so it would seem it is overfitting to the jumping behavior, possibly as a result of the decreased replay buffer size.

## 6.2 FRUITBOT ANALYSIS

Fruitbot performed least well of our experiments, so we dive in further to understand the dynamics at play.

**Module Count Ablation:** We first discuss the difference in expected return when we vary the number of modules for SANE, as visualized in Figure 7. Overall, we observe that the fewer the modules, the higher the maximum scores received. The one exception is Env 3, where 8 and 16 modules both receive comparable scores. However, in general the fewer the modules the more forgetting is observed as well. This is particularly noticeable on Envs 0, 1, and 4, with more ambiguity on Envs 2 and 3.

As we observed in the analysis of Climber, when a new task is switched to, we don’t create just a single module. Rather, the critic steadily learns to adapt to the new task; each time it passes the  $v^{LCB}$  threshold, a new module is created. Once the maximum number of modules has been reached, this triggers a merge. Since a merge combines the replay buffers of the two modules, when two “compatible” modules are merged, the resulting policy is more robust than that of the individual modules. However when two modules representing conflicting behaviors are merged, we see a reduction in performance. Taken together, this means that as merging is occurring, more modules in the ensemble will generally be more stable over time, but might be slower to learn. We discuss a concrete example of this in Section 6.2.1 below.

### 6.2.1 SINGLE RUN

Here we analyze a single run of Fruitbot, which allows us to see in more detail the dynamics of SANE. We use an ensemble with 8 modules to simplify analysis. We focus on three important points, labeled A, B, and C in Figure 8. In all three cases the module the Environment is using switches to an older module.

At A (21M timesteps), Env 1 switches from using Module 193 to Module 10. By analyzing the Lineage plot (not shown here due to its large size) we see that 193 merged into Module 150, which then merged into Module 10. Thus the continued high performance on this task can be explained by a successful sequence of merges.

At B (27M timesteps), Env 2 switches from using Module 252 to Module 9. In this case, Module 252, which is a direct descendent of Module 9, merged into Module 197. Module 197 is at this point still a module available in the ensemble, meaning Env 2 began to activate a high-performing previous module (Module 9) instead of the result of the

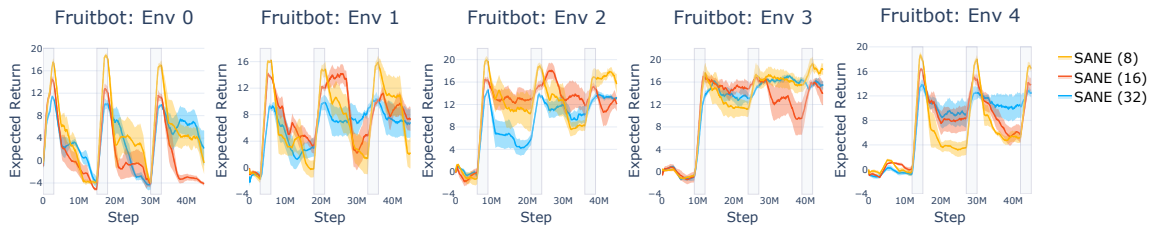


Figure 7: Comparison of SANE variations on the Fruitbot task sequence. The number in parentheses indicates the number of modules in the ensemble, ie. SANE (8) has 8 modules. Gray shaded rectangles show when the agent trains on each task.

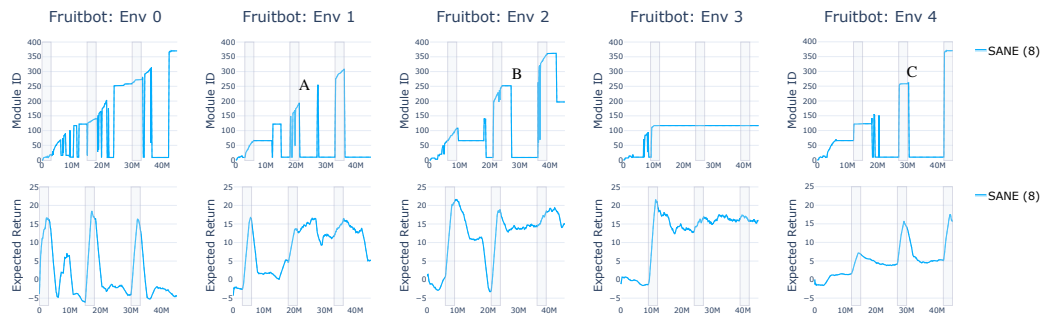


Figure 8: The Module ID and Expected Return plots for a single run of Fruitbot, aligned by timestep to see how modules are getting used and created while Fruitbot is training.

merge, implying that the critic value of 252 decayed as a result of its merger into Module 197. However, performance was rescued by return to a previous module and performance remains high.

At C (30M timesteps), Env 4 switches from using Module 261 to Module 10. Module 10, as we saw in case A, is a module that is well-suited for Env 1. In this case, Module 261 merged into Module 262, a descendent of Module 9, which as we saw in case B is well-suited for Env 2. Essentially, our 8 module ensemble lacks the capacity to adequately represent all of the behaviors necessary for this sequence of tasks, and start combining policies destructively, resulting in forgetting. This is mitigated by introducing more modules into our ensemble, as shown in Figure 7

## 7 CONCLUSION

Inspired by the fact that catastrophic forgetting is caused by updating all neurons in a network for all tasks, we propose the creation of self-activating modules to break up a network into modular components that only get updated when they are used. Our experimental results suggest that a dynamic ensemble, which creates modules as necessary and merges them to conserve resources, performs better than a static ensemble where all modules are created upfront. By combining these two novel features, we present SANE (Self-Activating Neural Ensembles) for continual reinforcement learning. We demonstrate SANE on sequences of Progen levels that prove particularly challenging for the current state-of-the-art (CLEAR), showing that our method reliably improves the mitigation of catastrophic forgetting. Furthermore, we present a thorough analysis of SANE, showing how modules are created, used, and merged on individual runs of Climber and Fruitbot, to provide a more comprehensive view into the system.

**Limitations and future directions** In this paper, we present a straightforward and simple instantiation of SANE, which has some limitations. First, using the initial observation of the episode to choose which module to activate limits the current method to tasks that are distinguishable immediately. Second, the complete separation of modules precludes transfer, wherein improvement on one task benefits performance on another. Future work to address these issues may include choosing the active module every  $n$  steps instead of once at the beginning of an episode, or making a hierarchical version of SANE where similar tasks activate similar paths through the tree while distinct tasks activate non-overlapping paths.

## ACKNOWLEDGEMENTS

This work was supported by ONR MURI, ONR Young Investigator Program, and DARPA MCS.

## REFERENCES

- Wickliffe C. Abraham and Anthony Robins. Memory retention—the synaptic stability versus plasticity dilemma. *Trends in neurosciences*, 28(2):73–78, 2005.
- Rahaf Aljundi, Punarjay Chakravarty, and Tinne Tuytelaars. Expert gate: Lifelong learning with a network of experts. In *Proceedings of the IEEE Conference on Computer Vision and Pattern Recognition*, pp. 3366–3375, 2017.
- Rahaf Aljundi, Francesca Babiloni, Mohamed Elhoseiny, Marcus Rohrbach, and Tinne Tuytelaars. Memory aware synapses: Learning what (not) to forget. In *Proceedings of the European Conference on Computer Vision (ECCV)*, pp. 139–154, 2018.
- Rahaf Aljundi, Eugene Belilovsky, Tinne Tuytelaars, Laurent Charlin, Massimo Caccia, Min Lin, and Lucas Page-Caccia. Online continual learning with maximal interfered retrieval. *Advances in neural information processing systems*, 32, 2019a.
- Rahaf Aljundi, Klaas Kelchtermans, and Tinne Tuytelaars. Task-free continual learning. In *Proceedings of the IEEE/CVF Conference on Computer Vision and Pattern Recognition*, pp. 11254–11263, 2019b.
- Oron Anschel, Nir Baram, and Nahum Shimkin. Averaged-dqn: Variance reduction and stabilization for deep reinforcement learning. In *International conference on machine learning*, pp. 176–185. PMLR, 2017.
- Emma Brunskill and Lihong Li. Pac-inspired option discovery in lifelong reinforcement learning. In *International conference on machine learning*, pp. 316–324. PMLR, 2014.
- Cristian Buciluă, Rich Caruana, and Alexandru Niculescu-Mizil. Model compression. In *Proceedings of the 12th ACM SIGKDD international conference on Knowledge discovery and data mining*, pp. 535–541, 2006.
- Lucas Caccia, Eugene Belilovsky, Massimo Caccia, and Joelle Pineau. Online learned continual compression with adaptive quantization modules. In *International Conference on Machine Learning*, pp. 1240–1250. PMLR, 2020.
- Hugo Caselles-Dupré, Michael Garcia-Ortiz, and David Filliat. S-trigger: Continual state representation learning via self-triggered generative replay. In *2021 International Joint Conference on Neural Networks (IJCNN)*, pp. 1–7. IEEE, 2021.
- Arslan Chaudhry, Puneet K Dokania, Thalaiyasingam Ajanthan, and Philip HS Torr. Riemannian walk for incremental learning: Understanding forgetting and intransigence. In *Proceedings of the European Conference on Computer Vision (ECCV)*, pp. 532–547, 2018a.
- Arslan Chaudhry, Marc’ Aurelio Ranzato, Marcus Rohrbach, and Mohamed Elhoseiny. Efficient lifelong learning with a-gem. In *International Conference on Learning Representations*, 2018b.
- Brian Cheung, Alexander Terekhov, Yubei Chen, Pulkit Agrawal, and Bruno Olshausen. Superposition of many models into one. *Advances in neural information processing systems*, 32, 2019.
- Karl Cobbe, Chris Hesse, Jacob Hilton, and John Schulman. Leveraging procedural generation to benchmark reinforcement learning. In *International conference on machine learning*, pp. 2048–2056. PMLR, 2020.
- Corinna Cortes, Xavier Gonzalvo, Vitaly Kuznetsov, Mehryar Mohri, and Scott Yang. Adanet: Adaptive structural learning of artificial neural networks. In *International conference on machine learning*, pp. 874–883. PMLR, 2017.
- Peter Dayan and Geoffrey E Hinton. Feudal reinforcement learning. volume 5, 1992.
- Thomas G Dietterich. Hierarchical reinforcement learning with the maxq value function decomposition. *Journal of artificial intelligence research*, 13:227–303, 2000.
- Timothy J Draelos, Nadine E Miner, Christopher C Lamb, Jonathan A Cox, Craig M Vineyard, Kristofor D Carlson, William M Severa, Conrad D James, and James B Aimone. Neurogenesis deep learning: Extending deep networks to accommodate new classes. In *2017 International Joint Conference on Neural Networks (IJCNN)*, pp. 526–533. IEEE, 2017.

- Lasse Espeholt, Hubert Soyer, Remi Munos, Karen Simonyan, Vlad Mnih, Tom Ward, Yotam Doron, Vlad Firoiu, Tim Harley, Iain Dunning, et al. Impala: Scalable distributed deep-rl with importance weighted actor-learner architectures. In *International Conference on Machine Learning*, pp. 1407–1416. PMLR, 2018.
- Chrisantha Fernando, Dylan Banarse, Charles Blundell, Yori Zwols, David Ha, Andrei A Rusu, Alexander Pritzel, and Daan Wierstra. Pathnet: Evolution channels gradient descent in super neural networks. *arXiv preprint arXiv:1701.08734*, 2017.
- Robert M French. Pseudo-recurrent connectionist networks: An approach to the ‘sensitivity-stability’ dilemma. *Connection science*, 9(4):353–380, 1997.
- Robert M French. Catastrophic forgetting in connectionist networks. *Trends in cognitive sciences*, 3(4):128–135, 1999.
- Scott Fujimoto, Herke Hoof, and David Meger. Addressing function approximation error in actor-critic methods. In *International conference on machine learning*, pp. 1587–1596. PMLR, 2018.
- Tommaso Furlanello, Jiaping Zhao, Andrew M Saxe, Laurent Itti, and Bosco S Tjan. Active long term memory networks. *arXiv preprint arXiv:1606.02355*, 2016.
- Alexander Gepperth and Cem Karaoguz. A bio-inspired incremental learning architecture for applied perceptual problems. *Cognitive Computation*, 8(5):924–934, 2016.
- Anirudh Goyal, Shagun Sodhani, Jonathan Binas, Xue Bin Peng, Sergey Levine, and Yoshua Bengio. Reinforcement learning with competitive ensembles of information-constrained primitives. In *International Conference on Learning Representations*, 2019.
- Stephen Grossberg. How does a brain build a cognitive code? In *Studies of mind and brain*, pp. 1–52. Springer, 1982.
- Abner Guzman-Rivera, Dhruv Batra, and Pushmeet Kohli. Multiple choice learning: Learning to produce multiple structured outputs. *Advances in neural information processing systems*, 25, 2012.
- Xu He and Herbert Jaeger. Overcoming catastrophic interference using conceptor-aided backpropagation. In *International Conference on Learning Representations*, 2018.
- Geoffrey Hinton, Oriol Vinyals, Jeff Dean, et al. Distilling the knowledge in a neural network. *arXiv preprint arXiv:1503.02531*, 2(7), 2015.
- David Isele and Akansel Cosgun. Selective experience replay for lifelong learning. In *Proceedings of the AAAI Conference on Artificial Intelligence*, volume 32, 2018.
- Pavel Izmailov, Dmitrii Podoprikin, Timur Garipov, Dmitry Vetrov, and Andrew Gordon Wilson. Averaging weights leads to wider optima and better generalization. In *34th Conference on Uncertainty in Artificial Intelligence 2018, UAI 2018*, pp. 876–885. Association For Uncertainty in Artificial Intelligence (AUAI), 2018.
- Robert A Jacobs, Michael I Jordan, Steven J Nowlan, and Geoffrey E Hinton. Adaptive mixtures of local experts. *Neural computation*, 3(1):79–87, 1991.
- Herbert Jaeger. Using conceptors to manage neural long-term memories for temporal patterns. *The Journal of Machine Learning Research*, 18(1):387–429, 2017.
- Nitin Kamra, Umang Gupta, and Yan Liu. Deep generative dual memory network for continual learning. *arXiv preprint arXiv:1710.10368*, 2017.
- Christos Kaplanis, Murray Shanahan, and Claudia Clopath. Policy consolidation for continual reinforcement learning. In *International Conference on Machine Learning*, pp. 3242–3251. PMLR, 2019.
- Ronald Kemker and Christopher Kanan. Fearnnet: Brain-inspired model for incremental learning. In *International Conference on Learning Representations*, 2018.
- Ronald Kemker, Marc McClure, Angelina Abitino, Tyler Hayes, and Christopher Kanan. Measuring catastrophic forgetting in neural networks. In *Proceedings of the AAAI Conference on Artificial Intelligence*, volume 32, 2018.
- Samuel Kessler, Jack Parker-Holder, Philip Ball, Stefan Zohren, and Stephen J Roberts. Same state, different task: Continual reinforcement learning without interference. *arXiv preprint arXiv:2106.02940*, 2021.

- James Kirkpatrick, Razvan Pascanu, Neil Rabinowitz, Joel Veness, Guillaume Desjardins, Andrei A Rusu, Kieran Milan, John Quan, Tiago Ramalho, Agnieszka Grabska-Barwinska, et al. Overcoming catastrophic forgetting in neural networks. *Proceedings of the national academy of sciences*, 114(13):3521–3526, 2017.
- Balaji Lakshminarayanan, Alexander Pritzel, and Charles Blundell. Simple and scalable predictive uncertainty estimation using deep ensembles. *Advances in neural information processing systems*, 30, 2017.
- Kimin Lee, Changho Hwang, KyoungSoo Park, and Jinwoo Shin. Confident multiple choice learning. In *International Conference on Machine Learning*, pp. 2014–2023. PMLR, 2017a.
- Sang-Woo Lee, Jin-Hwa Kim, Jaehyun Jun, Jung-Woo Ha, and Byoung-Tak Zhang. Overcoming catastrophic forgetting by incremental moment matching. *Advances in neural information processing systems*, 30, 2017b.
- Soochan Lee, Junsoo Ha, Dongsu Zhang, and Gunhee Kim. A neural dirichlet process mixture model for task-free continual learning. In *International Conference on Learning Representations*, 2019.
- Stefan Lee, Senthil Purushwalkam Shiva Prakash, Michael Cogswell, Viresh Ranjan, David Crandall, and Dhruv Batra. Stochastic multiple choice learning for training diverse deep ensembles. *Advances in Neural Information Processing Systems*, 29, 2016.
- Timothée Lesort, Hugo Caselles-Dupré, Michael Garcia-Ortiz, Andrei Stoian, and David Filliat. Generative models from the perspective of continual learning. In *2019 International Joint Conference on Neural Networks (IJCNN)*, pp. 1–8. IEEE, 2019.
- Timothée Lesort, Vincenzo Lomonaco, Andrei Stoian, Davide Maltoni, David Filliat, and Natalia Díaz-Rodríguez. Continual learning for robotics: Definition, framework, learning strategies, opportunities and challenges. *Information fusion*, 58:52–68, 2020.
- Stephan Lewandowsky and Shu-Chen Li. Catastrophic interference in neural networks: Causes, solutions, and data. In *Interference and inhibition in cognition*, pp. 329–361. Elsevier, 1995.
- Zhizhong Li and Derek Hoiem. Learning without forgetting. *IEEE transactions on pattern analysis and machine intelligence*, 40(12):2935–2947, 2017.
- Timothy P Lillicrap, Jonathan J Hunt, Alexander Pritzel, Nicolas Heess, Tom Erez, Yuval Tassa, David Silver, and Daan Wierstra. Continuous control with deep reinforcement learning. In *International Conference on Learning Representations*, 2016.
- Vincenzo Lomonaco, Karan Desai, Eugenio Culurciello, and Davide Maltoni. Continual reinforcement learning in 3d non-stationary environments. In *Proceedings of the IEEE/CVF Conference on Computer Vision and Pattern Recognition Workshops*, pp. 248–249, 2020.
- David Lopez-Paz and Marc’Aurelio Ranzato. Gradient episodic memory for continual learning. *Advances in neural information processing systems*, 30, 2017.
- Arun Mallya and Svetlana Lazebnik. Packnet: Adding multiple tasks to a single network by iterative pruning. In *Proceedings of the IEEE conference on Computer Vision and Pattern Recognition*, pp. 7765–7773, 2018.
- Arun Mallya, Dillon Davis, and Svetlana Lazebnik. Piggyback: Adapting a single network to multiple tasks by learning to mask weights. In *Proceedings of the European Conference on Computer Vision (ECCV)*, pp. 67–82, 2018.
- Michael McCloskey and Neal J Cohen. Catastrophic interference in connectionist networks: The sequential learning problem. In *Psychology of learning and motivation*, volume 24, pp. 109–165. Elsevier, 1989.
- Martial Mermillod, Aurélie Bugaiska, and Patrick Bonin. The stability-plasticity dilemma: Investigating the continuum from catastrophic forgetting to age-limited learning effects. *Frontiers in psychology*, 4:504, 2013.
- Volodymyr Mnih, Koray Kavukcuoglu, David Silver, Andrei A Rusu, Joel Veness, Marc G Bellemare, Alex Graves, Martin Riedmiller, Andreas K Fidjeland, Georg Ostrovski, et al. Human-level control through deep reinforcement learning. *nature*, 518(7540):529–533, 2015.
- Martin Mundt, Yong Won Hong, Iuliia Pliushch, and Visvanathan Ramesh. A wholistic view of continual learning with deep neural networks: Forgotten lessons and the bridge to active and open world learning. *arXiv preprint arXiv:2009.01797*, 2020.

- Oleksiy Ostapenko, Pau Rodriguez, Massimo Caccia, and Laurent Charlin. Continual learning via local module composition. *Advances in Neural Information Processing Systems*, 34, 2021.
- Giambattista Parascandolo, Niki Kilbertus, Mateo Rojas-Carulla, and Bernhard Schölkopf. Learning independent causal mechanisms. In *International Conference on Machine Learning*, pp. 4036–4044. PMLR, 2018.
- German I Parisi, Jun Tani, Cornelius Weber, and Stefan Wermter. Lifelong learning of spatiotemporal representations with dual-memory recurrent self-organization. *Frontiers in neurobotics*, pp. 78, 2018.
- German I Parisi, Ronald Kemker, Jose L Part, Christopher Kanan, and Stefan Wermter. Continual lifelong learning with neural networks: A review. *Neural Networks*, 113:54–71, 2019.
- Dongmin Park, Seokil Hong, Bohyung Han, and Kyoung Mu Lee. Continual learning by asymmetric loss approximation with single-side overestimation. In *Proceedings of the IEEE/CVF International Conference on Computer Vision*, pp. 3335–3344, 2019.
- Deepak Pathak, Dhiraj Gandhi, and Abhinav Gupta. Self-supervised exploration via disagreement. In *International conference on machine learning*, pp. 5062–5071. PMLR, 2019.
- Boris T Polyak and Anatoli B Juditsky. Acceleration of stochastic approximation by averaging. *SIAM journal on control and optimization*, 30(4):838–855, 1992.
- Sam Powers, Eliot Xing, Eric Kolve, Roozbeh Mottaghi, and Abhinav Gupta. Cora: Benchmarks, baselines, and metrics as a platform for continual reinforcement learning agents. *arXiv preprint arXiv:2110.10067*, 2021.
- Roger Ratcliff. Connectionist models of recognition memory: constraints imposed by learning and forgetting functions. *Psychological review*, 97(2):285, 1990.
- Sylvestre-Alvise Rebuffi, Alexander Kolesnikov, Georg Sperl, and Christoph H Lampert. icarl: Incremental classifier and representation learning. In *Proceedings of the IEEE conference on Computer Vision and Pattern Recognition*, pp. 2001–2010, 2017.
- Matthew Riemer, Ignacio Cases, Robert Ajemian, Miao Liu, Irina Rish, Yuhai Tu, and Gerald Tesauero. Learning to learn without forgetting by maximizing transfer and minimizing interference. In *International Conference on Learning Representations*, 2018.
- Mark B Ring. Child: A first step towards continual learning. In *Learning to learn*, pp. 261–292. Springer, 1998.
- Hippolyt Ritter, Aleksandar Botev, and David Barber. Online structured laplace approximations for overcoming catastrophic forgetting. *Advances in Neural Information Processing Systems*, 31, 2018.
- Anthony Robins. Catastrophic forgetting, rehearsal and pseudorehearsal. *Connection Science*, 7(2):123–146, 1995.
- David Rolnick, Arun Ahuja, Jonathan Schwarz, Timothy Lillicrap, and Gregory Wayne. Experience replay for continual learning. *Advances in Neural Information Processing Systems*, 32, 2019.
- David Ruppert. Efficient estimations from a slowly convergent robbins-monro process. Technical report, Cornell University Operations Research and Industrial Engineering, 1988.
- Andrei A Rusu, Sergio Gomez Colmenarejo, Caglar Gulcehre, Guillaume Desjardins, James Kirkpatrick, Razvan Pascanu, Volodymyr Mnih, Koray Kavukcuoglu, and Raia Hadsell. Policy distillation. *arXiv preprint arXiv:1511.06295*, 2015.
- Andrei A Rusu, Neil C Rabinowitz, Guillaume Desjardins, Hubert Soyer, James Kirkpatrick, Koray Kavukcuoglu, Razvan Pascanu, and Raia Hadsell. Progressive neural networks. *arXiv preprint arXiv:1606.04671*, 2016.
- Jonathan Schwarz, Wojciech Czarnecki, Jelena Luketina, Agnieszka Grabska-Barwinska, Yee Whye Teh, Razvan Pascanu, and Raia Hadsell. Progress & compress: A scalable framework for continual learning. In *International Conference on Machine Learning*, pp. 4528–4537, 2018.
- Younggyo Seo, Kimin Lee, Ignasi Clavera Gilaberte, Thanard Kurutach, Jinwoo Shin, and Pieter Abbeel. Trajectory-wise multiple choice learning for dynamics generalization in reinforcement learning. *Advances in Neural Information Processing Systems*, 33:12968–12979, 2020.

- Joan Serra, Didac Suris, Marius Miron, and Alexandros Karatzoglou. Overcoming catastrophic forgetting with hard attention to the task. In *International Conference on Machine Learning*, pp. 4548–4557. PMLR, 2018.
- Noam Shazeer, Azalia Mirhoseini, Krzysztof Maziarz, Andy Davis, Quoc Le, Geoffrey Hinton, and Jeff Dean. Outrageously large neural networks: The sparsely-gated mixture-of-experts layer. In *International Conference on Learning Representations*, 2017.
- Hanul Shin, Jung Kwon Lee, Jaehong Kim, and Jiwon Kim. Continual learning with deep generative replay. *Advances in neural information processing systems*, 30, 2017.
- Andrea Soltoggio, Kenneth O Stanley, and Sebastian Risi. Born to learn: the inspiration, progress, and future of evolved plastic artificial neural networks. *Neural Networks*, 108:48–67, 2018.
- Rupesh K Srivastava, Klaus Greff, and Jürgen Schmidhuber. Training very deep networks. *Advances in neural information processing systems*, 28, 2015.
- Richard S Sutton, Doina Precup, and Satinder Singh. Between mdps and semi-mdps: A framework for temporal abstraction in reinforcement learning. *Artificial intelligence*, 112(1-2):181–211, 1999.
- Yee Teh, Victor Bapst, Wojciech M Czarnecki, John Quan, James Kirkpatrick, Raia Hadsell, Nicolas Heess, and Razvan Pascanu. Distral: Robust multitask reinforcement learning. *Advances in neural information processing systems*, 30, 2017.
- Alexander V Terekhov, Guglielmo Montone, and J Kevin O’Regan. Knowledge transfer in deep block-modular neural networks. In *Conference on Biomimetic and Biohybrid Systems*, pp. 268–279. Springer, 2015.
- Chen Tessler, Shahar Givony, Tom Zahavy, Daniel Mankowitz, and Shie Mannor. A deep hierarchical approach to lifelong learning in minecraft. In *Proceedings of the AAAI Conference on Artificial Intelligence*, volume 31, 2017.
- Sebastian Thrun and Tom M Mitchell. Lifelong robot learning. *Robotics and autonomous systems*, 15(1-2):25–46, 1995.
- René Traoré, Hugo Caselles-Dupré, Timothée Lesort, Te Sun, Natalia Díaz-Rodríguez, and David Filliat. Continual reinforcement learning deployed in real-life using policy distillation and sim2real transfer. In *ICML Workshop on “Multi-Task and Lifelong Reinforcement Learning”*, 2019.
- Gido M Van de Ven and Andreas S Tolias. Generative replay with feedback connections as a general strategy for continual learning. *arXiv preprint arXiv:1809.10635*, 2018.
- Hado Van Hasselt, Arthur Guez, and David Silver. Deep reinforcement learning with double q-learning. In *Proceedings of the AAAI conference on artificial intelligence*, volume 30, 2016.
- Joel Veness, Tor Lattimore, David Budden, Avishkar Bhoopchand, Christopher Mattern, Agnieszka Grabska-Barwinska, Eren Sezener, Jianan Wang, Peter Toth, Simon Schmitt, et al. Gated linear networks. In *Proceedings of the AAAI Conference on Artificial Intelligence*, volume 35, pp. 10015–10023, 2021.
- Yeming Wen, Dustin Tran, and Jimmy Ba. Batchensemble: an alternative approach to efficient ensemble and lifelong learning. In *International Conference on Learning Representations*, 2020.
- Chenshen Wu, Luis Herranz, Xialei Liu, Joost van de Weijer, Bogdan Raducanu, et al. Memory replay gans: Learning to generate new categories without forgetting. *Advances in Neural Information Processing Systems*, 31, 2018.
- Ye Xiang, Ying Fu, Pan Ji, and Hua Huang. Incremental learning using conditional adversarial networks. In *Proceedings of the IEEE/CVF International Conference on Computer Vision*, pp. 6619–6628, 2019.
- Tianjun Xiao, Jiaying Zhang, Kuiyuan Yang, Yuxin Peng, and Zheng Zhang. Error-driven incremental learning in deep convolutional neural network for large-scale image classification. In *Proceedings of the 22nd ACM international conference on Multimedia*, pp. 177–186, 2014.
- Ju Xu and Zhanxing Zhu. Reinforced continual learning. *Advances in Neural Information Processing Systems*, 31, 2018.
- Jaehong Yoon, Eunho Yang, Jeongtae Lee, and Sung Ju Hwang. Lifelong learning with dynamically expandable networks. In *International Conference on Learning Representations*, 2018.

Friedemann Zenke, Ben Poole, and Surya Ganguli. Continual learning through synaptic intelligence. In *International Conference on Machine Learning*, pp. 3987–3995. PMLR, 2017.

Chen Zeno, Itay Golan, Elad Hoffer, and Daniel Soudry. Task agnostic continual learning using online variational bayes. *arXiv preprint arXiv:1803.10123*, 2018.

Jesse Zhang, Haonan Yu, and Wei Xu. Hierarchical reinforcement learning by discovering intrinsic options. *arXiv preprint arXiv:2101.06521*, 2021.

Guanyu Zhou, Kihyuk Sohn, and Honglak Lee. Online incremental feature learning with denoising autoencoders. In *Artificial intelligence and statistics*, pp. 1453–1461. PMLR, 2012.



## A APPENDIX

## A.1 HYPERPARAMETERS

Here we give the hyperparameters for our methods; see the provided code for more details. For convenience, we put all parameters that vary between methods above the line, and those that are consistent below.

Hyperparameter	Shared				
Num. actors	16				
Learner threads	1				
Unroll length	32				
Grad clip	40				
Reward clip	[-1, 1]				
Normalize rewards	No				
Entropy cost	0.01				
Discount factor	0.99				
LSTM	No				
Network arch.	Nature CNN				
Learning rate	4e-4				
Optimizer	RMSProp				
	$\alpha = 0.99$				
	$\epsilon = 0.01$				
	$\mu = 0$				

Hyperparameter	(Climber & Miner)		(Fruitbot)		
	SANE	SANE	CLEAR	P&C	EWC
Batch size	2	2	2	18	2
Baseline cost	5.0	0.5	0.5	0.5	0.5
EWC $\lambda$				30	300
EWC, min task steps					2e5
Fisher samples				100	100
Normalize Fisher				Yes	No
Online EWC $\gamma$				0.99	
KL cost				1.0	
Policy cloning cost				0.1	
Value cloning cost				0.005	
Replay ratio	8	8		8	
Replay buffer size	50k	12.5k	400k		
	(per module)	(per module)			
Max num. modules	8	32			
$\alpha_{u,inf}$	1.0	1.0			
$\alpha_{u,create}$	0.1	0.1			
$\alpha_{l,create}$	10.0	0.5			
Critic cadence $T$	1000	10000			
Critic target update rate $\tau_V$	0.9	0.9			
Uncertainty cost $\mu$	1.0	0.1			

Table 2: Hyperparameters for all methods. The network architecture is the “Nature CNN” model (Mnih et al., 2015).

Note that there are two different  $\alpha$  parameters for SANE. One describes the parameter used for inference ( $\alpha_{u,inf}$ ) and the other describes the parameters used during module creation ( $\alpha_{x,create}$ ).

**Batch size** Since two of the methods augment the batch with more data (SANE and CLEAR), there is the question of how to size the batches of the other baselines (EWC, P&C) fairly. There are two ways to view it. The first is to equalize the total amount of data the optimizer sees per gradient step (i.e. since the augmented size is 18, collect a batch size of 18 for EWC and P&C). The second is to equalize the amount of new data the optimizer sees (i.e. 2 new trajectories are collected so use a batch size of 2 for EWC and P&C). We compare the differences in Figure 9. We can see that a smaller batch (i.e. training more often) results in learning the tasks more quickly, but the impact on recall is more ambiguous: on Env 0 the smaller batch size recalls less well, but it’s comparable on all other environments.

Worth noting also is that the smaller batch size takes considerably longer to train. Given these facts we have chosen to use the larger batch size for our EWC and P&C baselines.

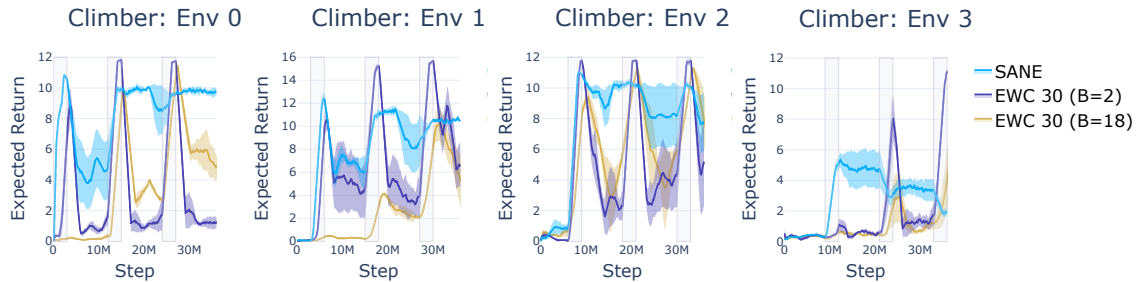


Figure 9: Comparison of running EWC with a batch size of 2 versus the default (18).

**Increasing network size** The base architecture used for all methods is the Nature CNN model (Mnih et al., 2015) with  $\sim 6e5$  parameters. To make the 8x version, we multiplied the number of filters at every convolutional layer by 6 (for a total of  $\sim 5.7e6$  parameters). We opted for making the network wider instead of deeper because: (i) conceptually this is more similar to the structure of the SANE ensemble (ii) it does not introduce the possibility of decreased performance due to gradient vanishing or exploding (Srivastava et al., 2015).

#### A.1.1 ARCHITECTURE OVERVIEW

Here we describe how SANE utilizes the highly parallel IMPALA method. Every SANE module is one instance of an IMPALA agent; all modules operate independently, with no shared parameters or data. Each IMPALA agent is composed of a set of actors that are constantly collecting data and populating a shared buffer with the results. When a separate learner thread detects that the minimum batch size of trajectories has been collected, it computes the losses and runs a gradient step. Not needing to pause the actors to update the model provides significant runtime improvements.

SANE augments this basic structure in one primary way. In order to switch modules, the currently running module is paused (all actors stop collecting data, and all learner threads stop updating the model) every  $s_{yield}$  seconds. At this point an activation score is computed for every module and the highest-scoring module is activated. Activation means that all actors are restarted, and model updating resumes. This alternating of module activation and data collection continues until all tasks are complete.

#### A.1.2 HYPERPARAMETER TUNING

First, we present the  $\lambda$  tuning graph for EWC in Figure 10. We ran using  $\lambda$  values in the range  $[1, 1e5]$  with a batch size of 18 ( $B=18$ ) on the Climber task sequence with 3 seeds. We also ran two experiments with ( $B=2$ ). We can see that while the lower  $\lambda$  values (1 and 10) learn the tasks better, they are also more inclined to forget, as can be seen particularly on Envs 0 and the first cycle of Env 2. Based on these results we chose  $\lambda = 300$  and a batch size of 2 for the experiments presented in the paper as the best balance of learning and remembering.

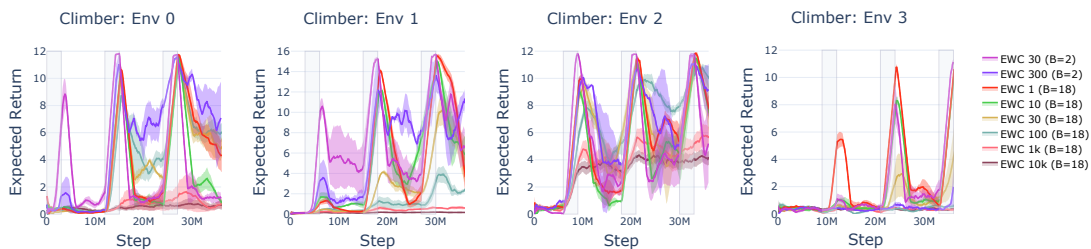


Figure 10: Comparison of EWC  $\lambda$  variations on the Climber task sequence. The number represents  $\lambda$ .

Second, we present the  $\lambda$  tuning graph for P&C in Figure 11, representing values in the range  $[3, 3e3]$ , over 3 seeds for a batch size of 18. We thus chose  $\lambda = 30$  for our experiments

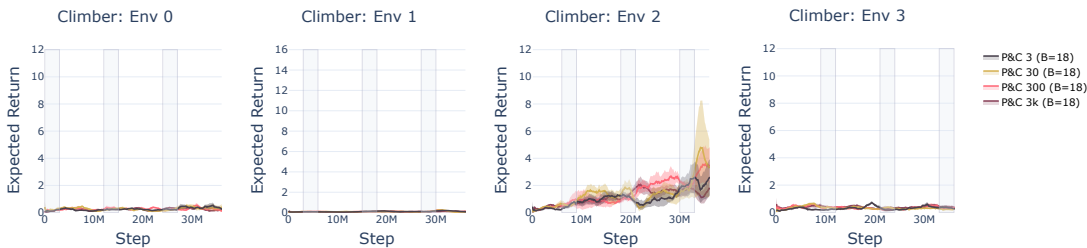


Figure 11: Comparison of P&C  $\lambda$  variations on the Climber task sequence. The number represents  $\lambda$ .

### A.2 PARAMETER ABLATION ON FRUITBOT

As shown in Table 2 we use different parameters for Climber/Miner vs Fruitbot. For simplicity we refer to the former set of parameters as SANE v1 and the latter as SANE v2.

Conceptually, the difference between SANE v1 and SANE v2 is that the former trains the critic more aggressively (higher coefficients and fewer frames between target network updates), but also has a much more conservative  $v_{LCB}$ , meaning more drift must be observed before a node is created. We observe that the former performed well on Climber and Miner, but on Fruitbot we obtained higher performance using the smoother critic training of SANE v2, as shown in Figure 12. However, it is worth noting that the ensemble learns and remembers in both cases, even when the parameters vary widely (e.g.  $\alpha_{l,create}$  differs by a factor of 20.). However, optimal parameter selection remains an area of future work.

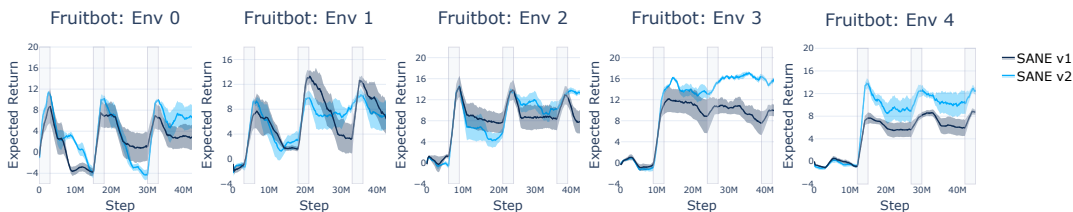


Figure 12: Comparison of SANE variations on the Fruitbot task sequence.

### A.3 LINEAGE PLOT, FRUITBOT

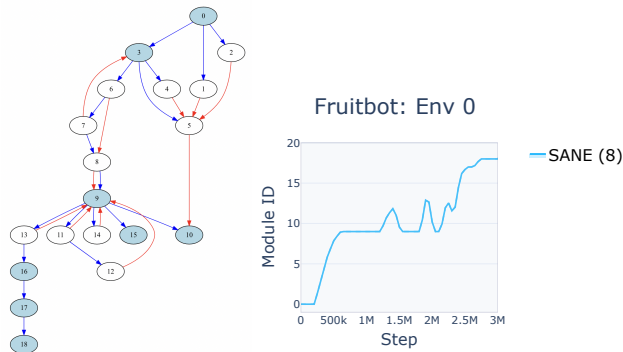


Figure 13: An example Lineage plot, showing how nodes are created and merged while training on Env 0 of Fruitbot.

While we are not able to provide the full Lineage plots used in the analysis above (a graph with hundreds of nodes displays poorly in pdf form), we show an example of what one looks like for the first task of Fruitbot. Node 0 is used initially, but soon spawns a cascading sequence of Nodes that settles for some time on Node 9. There is some churn as nodes are created but merged back into 9, until another burst of creation settles finally on Node 18, though we see in Figure 8 that this does not last either.

If the policies and critics improved monotonically, we would not see such a chaotic plot, but instead one more like what we see for Climber, in Figure 6. Essentially, since creation only happens when we detect that a node is worse than its anchor, this pattern of creation represents much noisier learning.

#### A.4 ALGORITHM PSEUDOCODE FOR SANE

---

##### Algorithm 1 SANE

---

**Require:** timestep  $t$ , total task timesteps  $T$ , state at episode start  $s_0$ , max allowed module count  $N$ , modules  $\mathcal{M} = \{M_1, \dots, M_k\}$  where  $M_i$  contains actor  $\pi_i$ , critic  $V_i$ , static anchor critic  $a_i$ , and replay buffer  $R_i$ .

- 1: **while**  $t < T$  **do**
- 2:    $M_{max} = \arg \max_i (v_{UCB,i}(s_0))$  ▷ select active module
- 3:   Collect  $t_{new}$  timesteps of data using  $M_{max}$
- 4:    $t := t + t_{new}$
- 5:
- 6:   **if**  $v_{UCB,M_{max}}(s) < v_a(s)$  **then** ▷ negative drift detected, so add module
- 7:
- 8:      $M_{new} := \text{clone}(M_{max})$
- 9:      $a_{new} := \text{clone}(V_{max})$
- 10:     $\mathcal{M} := \{M_1, \dots, M_k, M_{new}\}$
- 11:   **else**
- 12:     **if**  $v_{LCB,m}(s) > v_a(s)$  **then** ▷ positive drift detected, so update module
- 13:        $a_{max} := \text{clone}(V_{max})$
- 14:     **end if**
- 15:   **end if**
- 16:   **if**  $|\mathcal{M}| > N$  **then** ▷ merge modules
- 17:      $g_i := \text{avg}(\text{batch}(R_i)[\text{observation}])$  ▷ compute an avg observation for each module
- 18:      $M_i, M_j = \arg \min_{i,j} \|g_i, g_j\|_2$
- 19:      $M_{keep}, M_{remove} = \text{which of } M_i \text{ or } M_j \text{ has been used more and fewer times, respectively}$
- 20:      $R_{keep} = \{R_i, R_j\}$
- 21:      $\mathcal{M} = \mathcal{M} - M_{remove}$
- 22:
- 23:   **end if**
- 24: **end while**

---

#### A.5 FINAL AVERAGE PERFORMANCE TABLES

Task	SANE	Static SANE	CLEAR 8x	CLEAR	EWC 8x	PnC 8x	SANE Oracle
Env 0	<b>9.72 ± 0.29</b>	2.54 ± 1.85	3.02 ± 0.14	1.26 ± 0.08	7.46 ± 0.88	0.24 ± 0.06	9.52 ± 0.14
Env 1	10.43 ± 0.04	9.80 ± 0.49	2.34 ± 0.32	1.96 ± 0.21	<b>14.37 ± 1.09</b>	0.22 ± 0.05	10.02 ± 0.22
Env 2	7.82 ± 1.92	6.95 ± 1.77	1.08 ± 0.05	1.57 ± 0.43	<b>9.33 ± 0.91</b>	3.70 ± 0.95	10.66 ± 0.08
Env 3	1.99 ± 0.28	2.22 ± 0.34	7.46 ± 0.20	8.02 ± 0.26	<b>8.40 ± 0.42</b>	0.34 ± 0.05	2.71 ± 0.59

Table 3: Climber final average performance. The Oracle is not considered for the purposes of highlighting the average performance, as it is an idealized model.

Task	SANE	Static SANE	CLEAR 8x	CLEAR	EWC 8x	PnC 8x	SANE Oracle
Env 0	<b>10.25 ± 0.35</b>	6.61 ± 2.18	2.89 ± 0.24	2.35 ± 0.12	2.71 ± 0.26	2.03 ± 0.55	8.01 ± 1.41
Env 1	<b>12.43 ± 0.03</b>	8.25 ± 2.07	9.24 ± 0.71	4.90 ± 0.58	11.06 ± 0.68	3.46 ± 0.66	12.56 ± 0.06
Env 2	9.64 ± 2.09	9.46 ± 2.11	4.93 ± 0.42	3.90 ± 0.39	<b>10.65 ± 0.62</b>	2.11 ± 0.54	11.49 ± 0.22
Env 3	2.97 ± 0.05	3.06 ± 0.05	7.06 ± 2.31	10.74 ± 1.87	<b>12.96 ± 0.02</b>	1.93 ± 0.26	3.15 ± 0.06

Table 4: Miner final average performance. The Oracle is not considered for the purposes of highlighting the average performance, as it is an idealized model.

Task	SANE	Static SANE	CLEAR 8x	CLEAR	EWC 8x	PnC 8x	SANE Oracle
Env 0	2.18 ± 3.46	-0.70 ± 0.37	<b>3.77 ± 0.50</b>	-2.36 ± 0.24	2.05 ± 1.77	-2.09 ± 0.74	11.84 ± 0.68
Env 1	<b>6.71 ± 2.43</b>	2.45 ± 0.40	2.85 ± 0.45	1.26 ± 0.44	-0.91 ± 0.56	-2.08 ± 0.78	11.85 ± 0.47
Env 2	<b>13.13 ± 0.21</b>	10.34 ± 3.01	9.50 ± 0.52	5.87 ± 0.26	10.87 ± 2.73	4.89 ± 1.68	15.39 ± 1.71
Env 3	<b>15.38 ± 0.84</b>	6.80 ± 0.43	9.52 ± 0.66	6.73 ± 1.36	9.74 ± 2.51	1.16 ± 0.65	16.25 ± 0.88
Env 4	12.36 ± 0.72	19.48 ± 0.95	<b>23.86 ± 0.47</b>	19.84 ± 3.06	6.07 ± 0.94	1.37 ± 0.37	12.66 ± 0.75

Table 5: Fruitbot final average performance. The Oracle is not considered for the purposes of highlighting the average performance, as it is an idealized model.

## A.6 2 MODULE EXPERIMENTS

Here we present training SANE using only 2 modules (each with 2e5 replay buffer entries) on Climber. The intent of this experiment is to look at how having fewer modules than tasks impacts performance. We can see that while peak performance is generally higher, recall is poor overall. Perhaps unsurprisingly, the curve resembles that of CLEAR: reaching similar maximum values, and observing the same forgetting.

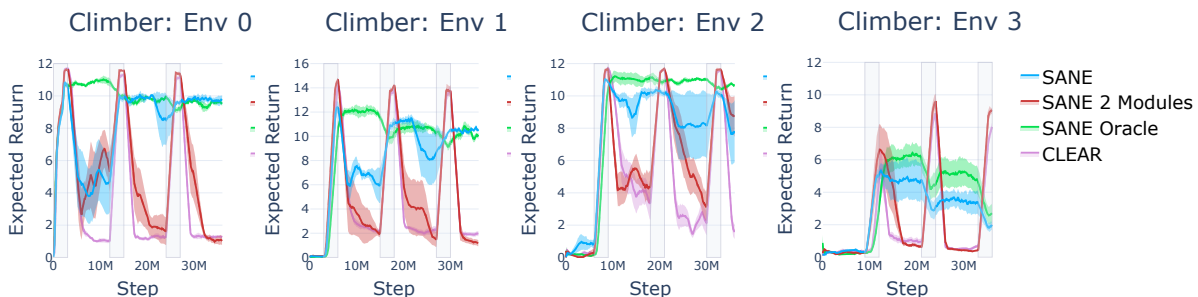


Figure 14: Comparison for using SANE with 2 modules to other SANE variants and CLEAR.

## A.7 EXTENDED BACKGROUND

In the standard, single-task reinforcement learning scenario, we consider the task  $\mathcal{T}$  as a discrete-time Markov Decision Process (MDP) consisting of a tuple  $\langle S, A, T, r, \gamma, \rho_0, \rangle$ , with state space  $S$ , action space  $A$ , state transition probability function  $T$ , reward function  $r$ , discount factor  $\gamma$ , and probability distribution  $\rho_0$  on the initial states  $S_0 \subset S$ . The goal is to learn a policy  $\pi(a|s)$  which maximizes the expected return, where the return  $R_t$  of a state  $s$  at timestep  $t$  is the discounted sum of rewards over an infinite-horizon trajectory from state  $s$ .

For continual RL (Kirkpatrick et al., 2017; Schwarz et al., 2018; Rolnick et al., 2019), we extend this setting by considering a sequence of  $N$  tasks,  $\mathcal{S}_N := (\mathcal{T}_1 \dots \mathcal{T}_N)$ , presented to the agent. This induces a non-stationary learning process as any component of the MDP may change on task switch. A capable continual RL agent should continue to learn new skills (maintain plasticity), recall prior learned behavior (mitigate catastrophic forgetting), and transfer old abilities to new domains (demonstrate forward transfer). We assume the agent trains on task  $\mathcal{T}_i$  at timesteps in the interval  $[A_i, B_i)$ , for  $k_i = B_i - A_i$  timesteps. Here  $A_i$  and  $B_i$  are the task boundaries denoting the start and end, respectively, of task  $\mathcal{T}_i$ . Additionally, we may cycle through the tasks  $M$  times, which yields full task sequence  $\mathcal{S}_{NM}$  that has length  $N \cdot M$ .

## A.8 ANALYSIS OF ESTIMATED RETURNS

In Figure 15 we present SANE’s estimated vtrace return in comparison to the observed vtrace return for the training periods for each task for a single run. There is a bit of overestimation in Env 0, more significant overestimation in Env 1, but almost none in Envs 2 and 3. Env 1 is also where we see the most uncertainty. Note that the first time a transition to a new task occurs, the estimated return is near zero.

We believe these estimates to be close enough that using our estimated vtrace returns is preferred over using a history of recent returns. An example of when this is the case is if every episode is different; then any window size to average over poses problems: the best module will not be activated and creation will not occur properly. Furthermore, we hope

to extend SANE such that activation occurs many times during an episode as well, so modules can capture even more fine-grained behaviors. This fine-grained behavior becomes impossible if we are reliant on final returns.



Figure 15: Comparison of the true and predicted vtrace returns.

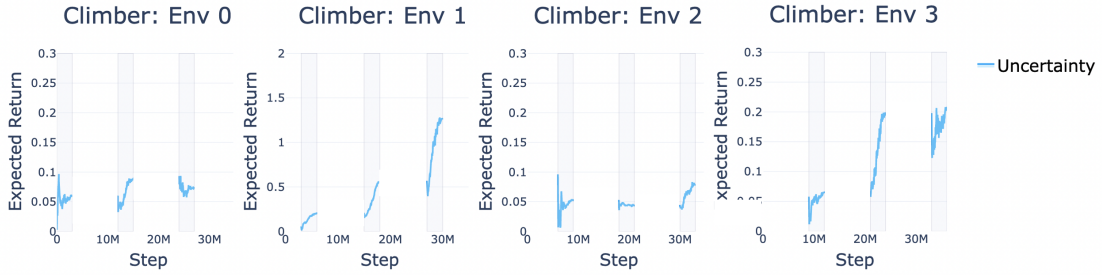


Figure 16: Graph of the uncertainty of SANE's prediction of our vtrace returns.